*International Journal of Engineering & Technology*, 7 (4.36) (2018) 426-431

International Journal of Engineering & Technology

*Website: www.sciencepubco.com/index.php/IJET*

***Research paper***

# Application of Wavelet Analysis in Tool Wear Evaluation Using Image Processing Method

**Lee Woon Kiow*, Syed Mohamad Aiman Tuan Muda, Ong Pauline, Sia Chee Kiong, Norfazillah Talib, Aslinda Saleh**

*Universiti Tun Hussein Onn Malaysia, 86400 Parit Raja, Batu Pahat, Johor Malaysia*
**Corresponding author E-mail:wklee@uthm.edu.my*

**Abstract**

Tool wear plays a significant role for proper planning and control of machining parameters to maintain the product quality. However, existing tool wear monitoring methods using sensor signals still have limitations. Since the cutting tool operates directly on the workpiece during machining process, the machined surface provides valuable information about the cutting tool condition. Therefore, the objective of present study is to evaluate the tool wear based on the workpiece profile signature by using wavelet analysis. The effect of wavelet families, scale of wavelet and statistical features of the continuous wavelet coefficient on the tool wear is studied. The surface profile of workpiece was captured using a DSLR camera. Invariant moment method was applied to extract the surface profile up to sub-pixel accuracy. The extracted surface profile was analyzed by using continuous wavelet transform (CWT) written in *MATLAB*. The results showed that average, RMS and peak to valley of CWT coefficients at all scale increased with tool wear. Peak to valley at higher scale is more sensitive to tool wear. Haar was found to be more effective and significant to correlate with tool wear with highest $R^2$ which is 0.9301.

***Keywords***: *Tool wear monitoring; workpiece profile; machine vision; continuous wavelet transform.*

## 1. Introduction

Tool wear is an unavoidable circumstances in the machining process and needs to be monitored because the worn tool significantly degrade surface finish and dimension accuracy and even can cause machine disruption when the tool suddenly fails. The end effective tool life is usually evaluated by flank wear as the flank wear progresses gradually and thus can be easily monitored. Monitoring of tool wear can be divided into two types. They are direct and indirect method. Direct method is usually implemented by optical instruments which is accomplished by directly evaluating the change in the geometry of the cutting inserts. The most common instrument used to measure the flank wear in the industry sector is tool maker's microscope. For several hundred to several thousand magnification, more advanced measuring equipment such as scanning electron microscope, scanning white light interference microscope are chosen when the analysis of micro or nano scale is needed. However, these equipment only feasible for offline measurement. Evaluation of tool wear only can be implemented when cutting tool removed from the machine.

Tool wear monitoring using CCD (charge-coupled device) camera with image processing techniques as direct method has seen developed rapidly and gained more attention in the past decades. In this method, the acquisition of the image of cutting tool is done by a CCD camera with appropriate illumination reflected on the plane of worn surface which without the need to dismantle the cutting tool from the machine. But, this method feasible only between the cutting operations. The image acquisition is not feasible for when there is in contact with the workpiece and is almost unachievable with the presence of coolant during the machining operation [1-3].

Indirect methods are based on sensor signals measured during the machining that can be correlated to tool condition. The main advantages of indirect method is that the tool state can be monitored in real time. In the past years, extensive research efforts have been devoted to online tool wear monitoring from the measureable sensor signal, for instance, cutting force, AE (acoustic emission), vibration, temperature, motor current, power consumption or a combination of them [4-7]. Multiple sensors enable to enrich the information as indicative of tool state and improve the accuracy of tool condition monitoring system. The sensor signal acquired from the machining operation need to be derived so that can be used to correlate the wear of cutting tool adequately. The average value, the root mean square (RMS), variance, kurtosis and skewness are the most common signal feature attributes derived from any time domain signal aims to reduce the high dimensionality of the sensor signal and to produce synthetic sensor signal characterization for correlating the tool conditions. The sensor signal in time domain can also be reconstructed into frequency domain and time-frequency domain using fast Fourier transform (FFT), short time Fourier transform (STFT) and wavelet transform. The amplitude of the dominant spectral peaks and wavelet coefficient are often used to correlate to the flank wear [8-10].

With the rapid development of artificial intelligence (AI) technology, various AI techniques have been employed for constructing tool wear monitoring models. The main AI techniques applied for monitoring tool condition are artificial neural networks (ANN), fuzzy logic, neuro-fuzzy inference systems, hidden Markov models, support vector machines (SVM) and etc [11]. Cutting parameters and additional factors such as the statistical features of sensor signals as inputs are vastly studied and have been receiving considerable attention nowadays. For example, Liao et al. [12] developed a hybrid hidden Markov model for monitoring the state of

cuting tool based on the analysis of cutting force. The wavelet coefficients of cutting force at various frequencies band as a cross-twist Markov depended structure able to describe the wear of tool from frequency dimension. Liu et al. [13] monitored tool state on the basis of cutting force and vibration using SVM. Wavelet decomposition is employed to extract the sensorial attributes including average and variances of the decomposed signals as the input vector. In recent work, Chen et al. [14] successfully correlate the flank wear using support vector regression, ANN and deep belief network based on the statistical features of cutting force, vibration and AE signal. Although indirect method seems promising, these sensors are rarely adopted by industry because they are significantly affected by environmental conditions. In addition, these methods are difficult to be implemented because assessment of some of unpredicted signals received from cutting process is not easy and the processing signals are stochastic in nature as well as the non-linear correlation between the measured sensorial features and tool wear which difficult to correlate each other.

The monitoring of cutting tool has also been achieved based on the machined surface quality because the cutting tool operates directly on the workpiece. As the machine vision and image processing methods develop rapidly, many research works in application of machine vision to evaluate tool state from the workpiece surface of a machined part has begun in the past. The sharp and dull tools can be distinguished based on the texture of a turned surface [15]. Danesh and Khalili [16] also proposed a method to determine tool wear from irregularities of surface texture. Undecimated wavelet transform was used to decompose the surface texture image into sub-images and was then analyzed by gray-level co-occurrence matrix (GLCM) to classify tool wear.

The variation of texture descriptors as indicator to identify tool wear gaining popularity in recent works. For instance, contrast and homogeneity obtained from surface texture images were successfully correlated with tool flank wear [17]. The Voronoi tessellation has been employed to extract the number of polygons with zero cross moment and the total void area of the Voronoi diagram from images of the machined surface [18]. It was found that Voronoi polygons was irregular when the flank wear increased. In recent year, Bhat et al. [19] developed a novel technique for classification of tool condition by using a kernel-based support vector machine method rest on the derived attributes obtained from the GLCM of machined surface. Similar work has also been done by Dutta et al. [20]. GLCM, Voronoi tessellation, and discrete wavelet transform based methods is proposed to extract the informative features from surface texture for evaluating the flank wear using SVM based regression models. Li and An [21] extracted the workpiece texture feature value in a texture window by using the entropy feature which determined by GLCM. Findings show entropy remains monotonic when tool wear increased. It can be observed that the surface textures can be effectively to monitor tool wear since it vary significantly as the tool wear. However, the illumination condition and the contamination and coolants on machined surface greatly influence the surface texture evaluation.

To overcome this limitation, previous studies showed the 2D images of the contour of the surface profile taken using CCD camera with assistance of backlight has successfully been used to assess the nose wear and the flank wear. This is because all predominant tool wears can have remarkable effects on the workpiece profile since nose radius has direct effect on the workpiece profile. The nose wear and flank wear were determined by subtracting the workpiece profile accomplished by worn tool from the workpiece profile generated by unworn tool [22-23]. The main disadvantage of this approach is difficult to overlap the workpiece profile precisely which greatly affects its accuracy. In present study, a vision based method is developed to evaluate the wear of cutting insert from the turned workpiece profile signature using continuous wavelet transform (CWT). Statistical wavelet coefficient of workpiece profile in different scale of the decomposed extracted surface profile was calculated to be correlated to flank wear.

## 2. Methodology

### 2.1. Experimental setup

The machining conditions is tabulated in Table 1. The machining was conducted using a *Harrison Alpha 400 CNC* lathe machine under dry cutting. A commercially available carbide tool (CNMG 120408N-GU Sumitomo, Ltd.) was used to turn the AISI 1045 carbon steel workpiece. Cutting speed of 200 mm/min, feed rate of 0.3 mm/rev and 0.5 mm depth of cut were used in the machining experiments. Measurement of flank wear were conducted by means of a tool maker's microscope (*Nikon MM-60*).

**Table 1:** Machining conditions

| | |
|---|---|
| Machine | *Harrison Alpha 400 CNC* |
| Cutting tool | Carbide insert (CNMG 120408N-GU Sumitomo, Ltd) |
| Workpiece material | AISI 1045 carbon steel |
| Cutting speed (rev/min) | 200 |
| Feed rate (mm/rev) | 0.3 |
| Depth of cut (mm) | 0.50 |

Fig. 1 shows the schematic diagram of the basic components of image acquisition setup which consists of a DSLR camera (*Canon D60*) with a picture resolution of 18 mega pixels. The DSLR camera was fitted with a 4X close-up lens and connected to a personal computer through a USB cable for obtaining the 2D images of surface profile. Backlighting was generated by using a fluorescent source to illuminate the silhouette of the workpiece.

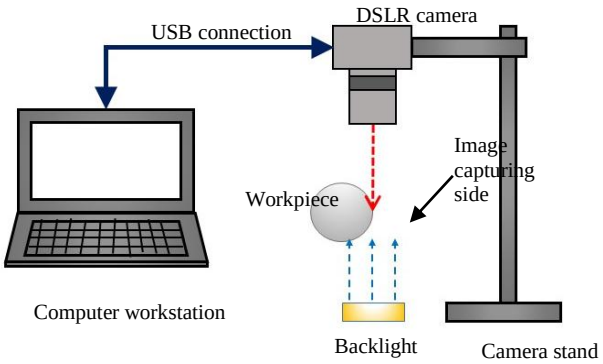


**Fig. 1:** Schematic diagram of image acquisition setup

### 2.2. Workpiece profile extraction procedure

The development of subpixel techniques for edge detection has gained more interest because the subpixel methods allow to overcome limitations due to the discrete structure of a pixel grid and it enables to locate the position of edge inside a pixel. In present study, an algorithm to locate the edge of workpiece profile with sub-pixel accuracy using moment invariant method was developed as illustrated in Fig. 2.

Firstly, the 2D image of workpiece profile was read as a RGB format. *MATLAB* command *'rgb2gray'* was used to convert the image from RGB to gray scale which is consisted of pixel intensity values that range from 0 (black) to 255 (white) bits. Wiener filtering was applied to remove the effect of the noise in the image. After that, the invariant moment method [24] was applied to determine the edge of workpiece profile to sub-pixel accuracy.

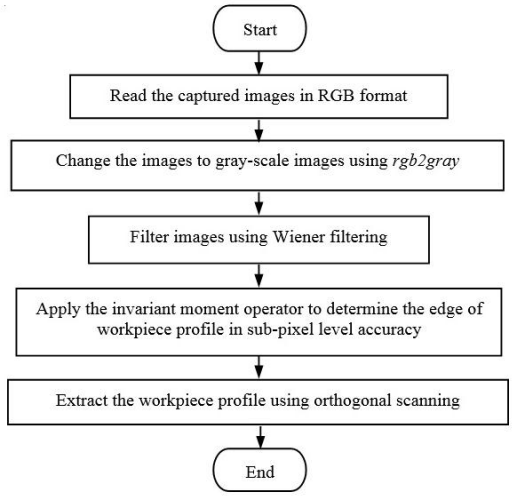


**Fig. 2:** surface profile detection algorithm

In the concept of invariant moment method, a sampled scan line across a step edge in the absence of noise is indicated by a set of pixel with intensity of $X_z$ where $z$ = 1, 2, 3 …, $N$. $S$ represents the optimal edge of the surface profile which is defined between a sequence of pixel's intensity $I_1$ followed by a sequence of pixel at another intensity $I_2$. Threshold independent method based on invariant moment equation is applied to calculate the first three grey level moments to the edge data $\overline{m_1}$ , $\overline{m_2}$ and $\overline{m_3}$ of the input data sequence in the grayscale as shown in Eq. (1):

$$\overline{m_i} = \frac{1}{N}\sum_{z=1}^{N}(X_z)^i \tag{1}$$

where $X_z$ is the intensity of the pixel in gray scale images, $i$ is integer number of 1, 2, 3 and $N$ represents total number of pixel within column $i$.

The first three moments of gray level brightness can be determined by:

$$\overline{m_i} = \sum_{j=1}^{2}\rho_j I_j^i \tag{2}$$

The brightness of $I_1$ and $I_2$ can be solved by:

$$I_1 = \overline{m}_1 - \lambda\sqrt{\frac{\rho_2}{\rho_1}} \tag{3}$$

$$I_2 = \overline{m}_1 + \lambda\sqrt{\frac{\rho_1}{\rho_2}} \tag{4}$$

$$\rho_2 = \frac{1}{2}\left[1+\alpha\sqrt{\frac{1}{4+\alpha^2}}\right] \tag{5}$$

where the densities of the brightness value are $\rho_1$ and $\rho_2$. The skewness of a set of data sequence, $\alpha$ can be determined in the Eq. (6):

$$\alpha = \frac{2\overline{m}_1 + \overline{m}_3 - 3\overline{m}_1\overline{m}_2}{\lambda^3} \tag{6}$$

where $\lambda$ is sample variance given by:

$$\lambda = \sqrt{\overline{m}_2 - \overline{m}_1^2} \tag{7}$$

The value of the gray level brightness densities are correlated by:

$$\rho_1 + \rho_2 = 1 \tag{8}$$

Thus, the optimal edge location of the surface profile in subpixel is calculated as shown in Eq. (9):

$$S = N\rho_1 \tag{9}$$

Orthogonal scanning algorithm developed in MATLAB was used to detect the contour of surface roughness profile. The $S$ value on the surface profile calculated from Eq. (9) was searched by the orthogonal scanning which starts from the first point of the first row of pixel of image. The contour of surface profile is produced when the scanning process had repeated continuously to locate entire subpixel $S$ value that located the surface profile at each column. A average value of the surface profile was then calculated by using least squares fitting. This aims to remove any tilt that appeared in the surface profile by subtracting each point on the detected profile from the mean line. Scaling factor was determined by using the known diameter pin gage in order to convert the profile of the workpiece from pixel unit to metric unit. The image of pin gage was captured by positioning the pin gage at the level of the axis of the workpiece that corresponds to the edge of the workpiece.

Table 1 and Table 2 tabulates the comparison results of arithmetic surface roughness parameter, $R_a$ and root mean square roughness parameter, $R_q$ obtained from proposed vision method and from mechanical stylus instrument, respectively. It can be observed that, the $R_a$, $R_q$ roughness parameters shows an error of only 4.26% and 4.17%, respectively. An error with 0-5% exceptionally good. The comparison shows the error is small (less than 5%) and thus the proposed machine vision method is able to provide a reliable workpiece profile to be used for analysis

**Table 2:** The experimental value and predicted value of $R_a$

| Cutting time | Stylus method | | | | Vision method | | | | Error (%) |
|---|---|---|---|---|---|---|---|---|---|
| (min) | 1 | 2 | 3 | average | 1 | 2 | 3 | average | |
| 1 | 3.32 | 3.56 | 3.45 | 3.44 | 3.24 | 3.29 | 3.43 | 3.32 | 3.23 |
| 2 | 3.31 | 3.51 | 3.55 | 3.42 | 3.42 | 3.11 | 3.02 | 3.18 | 7.05 |
| 3 | 3.26 | 3.41 | 3.33 | 3.48 | 3.06 | 3.36 | 3.63 | 3.35 | 3.69 |
| 4 | 3.54 | 3.46 | 3.32 | 3.44 | 3.01 | 3.27 | 3.46 | 3.25 | 5.62 |
| 5 | 3.55 | 3.87 | 4.16 | 3.86 | 3.66 | 3.53 | 4.20 | 3.79 | 1.70 |
| | | | | | | | | **MAPE (%)** | **4.26** |

**Table 3:** The experimental value and predicted value of $R_q$

| Cutting time | Stylus method | | | | Vision method | | | | Error (%) |
|---|---|---|---|---|---|---|---|---|---|
| (min) | 1 | 2 | 3 | average | 1 | 2 | 3 | average | |
| 1 | 3.94 | 4.01 | 3.85 | 3.93 | 3.81 | 3.67 | 3.97 | 3.82 | 2.91 |
| 2 | 3.72 | 4.15 | 4.08 | 3.98 | 3.90 | 3.62 | 3.51 | 3.68 | 7.76 |
| 3 | 3.77 | 3.92 | 3.81 | 3.83 | 3.58 | 3.79 | 4.02 | 3.80 | 1.06 |
| 4 | 4.03 | 3.98 | 3.83 | 3.95 | 3.53 | 3.65 | 3.91 | 3.69 | 6.39 |
| 5 | 4.05 | 4.29 | 4.46 | 4.27 | 4.09 | 3.94 | 4.42 | 4.15 | 2.74 |

| | | |
|---|---|---|
| **MAPE (%)** | **4.17** | |

**Table 4:** The Coefficient of determination, $R^2$

| Type of Wavelet | Average Value | | | RMS | | | Peak to Valley | | |
|---|---|---|---|---|---|---|---|---|---|
| | 20 | 60 | 100 | 20 | 60 | 100 | 20 | 60 | 100 |
| Morlet | 0.9020 | 0.9168 | 0.8158 | 0.9189 | 0.9274 | 0.9127 | 0.6344 | 0.8847 | 0.6726 |
| Mexican hat | 0.9109 | 0.6873 | 0.6350 | 0.9080 | 0.7518 | 0.5949 | 0.9250 | 0.8464 | 0.6815 |
| Haar | 0.8913 | 0.9240 | 0.7768 | 0.9122 | 0.9121 | 0.8618 | 0.1302 | 0.8881 | **0.9301** |
| Daubechies | 0.8790 | 0.9259 | 0.8359 | 0.8635 | 0.9058 | 0.8952 | 0.6341 | 0.8380 | 0.8771 |

### 2.3. Continuous wavelet analysis

Continuous wavelet transform (CWT) is applied to analyse the actual workpiece profile obtained from experiment. CWT is the most popular method for analysing the workpiece profile in time-frequency domain and it allows analysis of workpiece profile waveform on a local level, which is especially important when processing non-stationary workpiece profile resulted from tool wear. The CWT coefficient, $\kappa(a,b)$ was calculated by integral of the inner product of wavelet function, $\psi_{b,a}(t)$ and the workpiece profile waveform in time domain, $F(t)$ as shown in Eq. (10) [25]:

$$\kappa(a,b) = \int_{-\infty}^{\infty} F(t)\psi_{b,a}^{*}(t)dt \tag{10}$$

where $\psi_{b,a}(t)$ is the wavelet function and $*$ represents the complex conjugation. *a* is a scaling or dilation controlling the width of the wavelet function and *b* is a translation that controls the location of the wavelet. Transformation is based on the comparison between the wavelet function and the parts of workpiece profile waveform defined of equal width within a defined time interval. The size of the wavelet function $\psi_{b,a}(t)$ varies with the scaling is interpreted in Eq. (11). The transform process is achieved through continued scaling and translation of the wavelet function along the length of the surface profile. High similarity degree exists between the wavelet function and surface profile when the coefficients at that translation and scale are large and vice versa and therefore gives an indicative correlation of the frequency content of the surface profile. In this study, the Morlet, Mexican Hat, Haar and Daubechies wavelet were chosen to correlate with the flank wear.

$$\psi_{b,a}(t) = \frac{\psi}{\sqrt{a}}\left(\frac{t-b}{a}\right) \tag{11}$$

## 3. Results and discussions

These 4 types wavelet function with the statistical features which are mean average, root mean square (RMS) and peak to valley of CWT coefficients value was compared, in order to find the best correlation with the tool wear. Different of wavelet function can affected the CWT coefficient value and different CWT coefficient value can have a good or bad relation with the tool wear. In order of CWT to correlate the tool wear condition, the mean average, RMS and peak to valley of CWT coefficient value at low (20), medium (60) and high (100) scales was calculated and extracted. Fig. 3 to Fig. 6 show that the variation of mean, RMS and peak to valley of CWT coefficient of surface profile at scale of low, medium, and high for various wavelet function.

It can be observed that the average and RMS value of CWT coefficient increase consistently with the flank wear at different scale for each wavelet family. In contrast, the peak to valley of the CWT is also increases with the flank wear, but it fluctuates significantly which indicates that less agreement with the flank wear. This is because the peak to valley value are susceptible to disturbances. Fig. 3 to Fig. 6 show the comparison between each statistical feature at different scale (20, 60 and 100) for each mother wavelet. As seen in figures, that peak to valley value is found to be more sensitive to flank wear compare to the average and RMS CWT coefficient. In addition, the results also indicate that higher scale, the CWT coefficients increases consistently with the flank wear. This is because of irregular surface profile or random features exist in the surface profile introduced other spatial frequencies after tool has worn [26]. Low spatial frequencies were observed was due to presence of the waviness which could be detected from the higher scale as scale is inversely proportional to frequency.

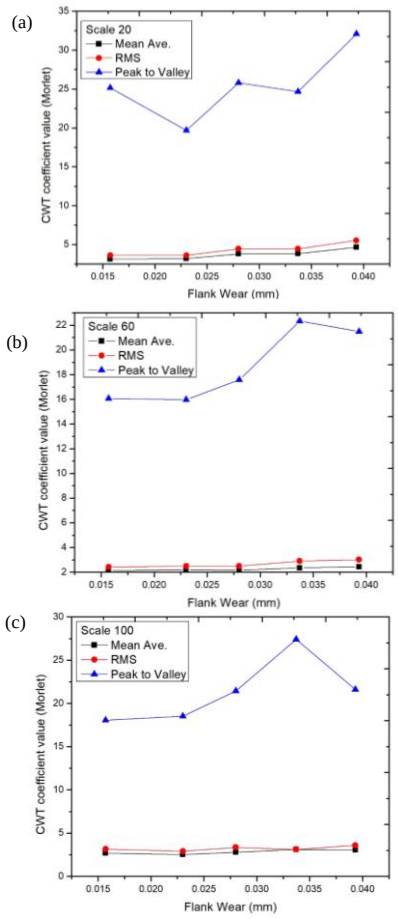


**Fig. 3:** CWT coefficient with Morlet wavelet at scale of (a) 20 (b) 60 and (c) 100

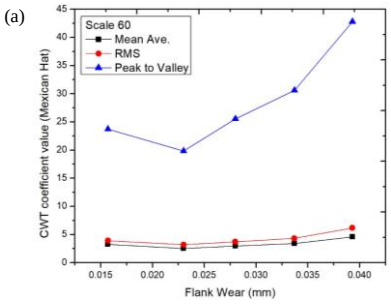

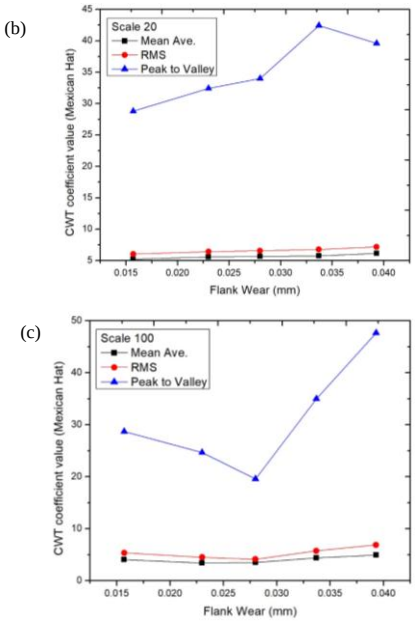


**Fig. 4:** CWT coefficient with Mexican Hat wavelet at scale of (a) 20 (b) 60 and (c) 100

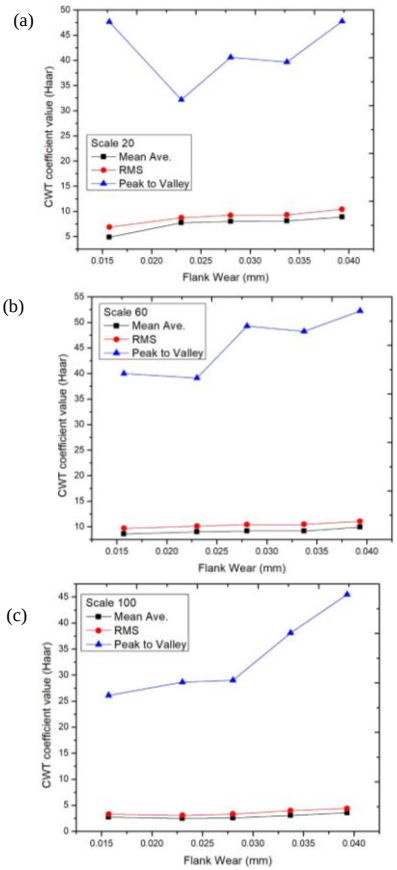


**Fig. 5:** CWT coefficient with Haar wavelet at scale of (a) 20 (b) 60 and (c) 100

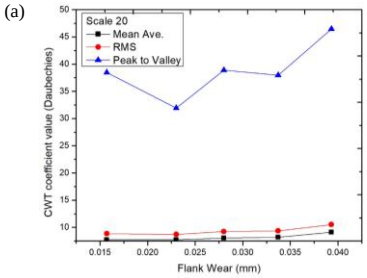


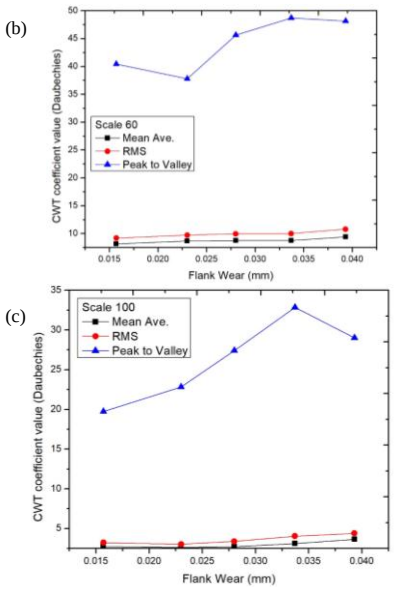


**Fig. 6:** CWT coefficient with Daubechies wavelet at scale of (a) 20 (b) 60 and (c) 100

The coefficient of determination or $R^2$ value for linear regression is calculated by fitting the trend of variation of statistical attributes derived from each wavelet function at each decomposition level and the variation of flank wear using linear regression. Table 4 presents the coefficient of determination $R^2$ for each value of statistical features. From the table, it can be concluded that Haar was found to be more effective and significant to correlate well with tool wear at higher scale because possess with the highest $R^2$ which is 0.9301.

## 4. Conclusion

A tool wear monitoring system from the workpiece profile signature coupled with vision method is proposed to evaluate the flank wear of cutting tools in turning. The extracted subpixel surface profile was analysed by using CWT and the statistical features of CWT coefficient from workpiece profile signature at different scale was extracted to examine the effects of tool wear on the surface profile signature. In conclusion, average, RMS and peak to valley of CWT coefficients at all scale increased with tool wear. Peak to valley at higher scale is more sensitive to tool wear. Haar was found to be more effective and significant to correlate with tool wear with highest $R^2$ which is 0.9301.

The biggest obstacle facing the implementation of in-process tool condition monitoring is the need for experimentation to determine threshold values to develop direct quantitative relationship which relates to tool state to implement effective tool changing strategies in unmanned manufacturing. More research work is needed for advances in pattern recognition and machine learning techniques to overcome this obstacle.

## Acknowledgement

The authors are grateful to Universiti Tun Hussein Onn Malaysia for financial support of RMC Research Fund and TIER 1 Research Grant H235

## References

[1] Wang, W.H., Hong, G.S. & Wong, Y.S. (2006). "Flank wear measurement by a threshold independent method with sub-pixel accuracy". *International Journal of Machine Tools and Manufacture, 46(2),* 199-207.

[2] Zhang, J., Zhang, C., Guo, S., & Zhou, L. (2012). "Research on tool wear detection based on machine vision in end milling process". *Production Engineering, 6(4),* 431-437.
[3] Chethan, Y.D., Ravindra, H.V., Krishne, Y.T., & Kumar, S.B. (2015). "Machine vision for tool status monitoring in Inconel 718 using Blob analysis". *Materials Today: Proceeding, 2(4-5),* 1841-1848.
[4] Teti, R., Jemielniak, K., O'Donnell, G., & Dornfeld, D. (2010). Advanced monitoring of machining operations. *CIRP Annals-Manufacturing Technology, 59(2),* 717-739.
[5] Jemielniak, K., Kossakowska, J., & Urbanski, T. (2011a). "Application of wavelet transform of acoustic emission and cutting force signals for tool condition monitoring in rough turning of Inconel 625". *Proceedings of the Institution of Mechanical Engineers, Part B: Journal of Engineering Manufacture, 225(1),* 123-129.
[6] Bhuiyan, M.S.H., Choudhury, I.A., & Dahari, M. (2014). "Monitoring the tool wear, surface roughness and chip formation occurrences using multiple sensors in turning". *Journal of Manufacturing Systems, 33(4),* 476-487.
[7] Zhang, K.F., Yuan, H.Q., & Nie, P. (2015). "A method for tool condition monitoring based on sensor fusion". *Journal of Intelligent Manufacturing, 26(5),*1011–1026.
[8] Yesilyurt, I. (2006). "End mill breakage detection using mean frequency analysis of scalogram". *International Journal of Machine Tool and Manufacture, 46(3-4),* 450-458.
[9] Kious, M., Ouahabi, A., Boudraa, M., Serra, R., & Cheknane, A. (2010). "Detection process approach of tool wear in high speed milling. *Measurement", 43(10),* 1439-1446.
[10] Fang, N., Pai, P.S., & Edwards, N. (2012). "Tool-edge wear and wavelet packet transform analysis in high speed machining of Inconel 718". *Journal of Mechanical Engineering, 58(3),* 191-202.
[11] Siddhpura, A., & Paurobally, R. (2013). "A review of flank wear prediction methods for tool condition monitoring in a turning process". *International Journal of Advanced Manufacturing Technology, 65(1),* 371-393.
[12] Liao, Z., Gao, D., Lu, Y., Lv, Z. (2016). "Multi-scale hybrid HMM for tool condition monitoring". *International Journal of Advanced Manufacturing Technology, 84*: 2437-2448.
[13] Liu, C., Li, Y., Zhou, G, Shen, W. (2016). "A sensor fusion and support vector machine based approach for recognition of complex machining conditions". *Journal of Intelligent Manufacturing, 28:* 1739-1752.
[14] Chen, Y., Jin, Y., Jiri, G. (2018). "Predicting tool wear with multi-sensor data using deep belief network". *The International Journal of Advanced Manufacturing Technology, 99,* 1917-1926.
[15] Kassim, A.A., Mannan, M.A., & Mian, Z. (2007). "Texture analysis methods for tool condition monitoring. *Image and Vision Computing", 25(7),* 1080-1090.
[16] Daneshm M., Khalili, K. (2015). "Determination of tool wear in turning process using undecimated wavelet transform and textural features". *Procedia Technology, 19,* 98-105
[17] Dutta, S., Datta, A., Chakladar, N.D., Pal, S.K., Mukhopadhyay, S., & Sen, R. (2012). "Detection of tool condition from the turned surface images using an accurate grey level co-occurrence technique." *Precision Engineering, 36(3),* 458-466.
[18] Datta, A., Dutta, S., Pal, S.K., & Sen, R. (2013). "Progressive cutting tool wear detection from machined surface images using Voronoi tessellation method". *Journal of Materials Processing Technology, 213(12),* 2339-2349.
[19] Bhat, N.N., Dutta, S., Vashisth, T., Pal, S., Pal, S.K., Sen, R. (2016). "Tool condition monitoring by SVM classification of machined surface images in turning.". *International Journal Advanced Manufacturing Technology, 83*:1487-1502.
[20] Dutta, S., Pal, S.K., & Sen, R. (2016). "On-machine tool prediction of flank wear from machined surface images using texture analyses and support vector regression". *Precision Engineering, 43,* 34-42.
[21] Li, L., & An, Q. (2016). "An in-depth study of tool wear monitoring technique based on image segmentation and texture analysis. *Measurement", 79,* 44-52.
[22] Shahabi, H.H., & Ratnam, M.M. (2009a). "In-cycle monitoring of tool nose wear and surface roughness of turned parts using machine vision". *International Journal of Advanced Manufacturing Technology, 40(11),* 1148-1157.
[23] Shahabi, H.H., & Ratnam, M.M. (2009b). "Assessment of flank wear and nose radius wear from workpience roughness profile in turning operation using machine vision". *International Journal of Advanced Manufacturing Technology, 43(1),* 11-21.
[24] Tabatabai, A.J., & Mitchell, R. (1984). "Edge location to sub-pixel values in digital imagery". *IEEE Transactions on Pattern Analysis and Machine Intelligence, 6(2),* 188-201.
[25] Leavey, C.M., James, M.N., Summerscales, J., & Sutton, R. (2003). "An introduction to wavelet transforms: a tutorial approach. *Insight Non-Destructive Testing and Condition Monitoring", 45(5),* 344-353.
[26] Cheung, C.F., & Lee, W.B. (2000). "A multi-spectrum analysis of surface roughness formation in ultra-precision machining". *Precision Engineering, 24(1),* 77-87.